

Suppressing Brake Vibrations by Deliberately Introduced Damping



Dominik Schmid, Nils Gräbner, Utz von Wagner, and Volker Mehrmann

1 Introduction

Brake vibrations are a typical example of Noise, Vibration, Harshness (NVH) problems in the automotive industry, dominating the development costs in several fields like brakes. The high-frequency brake vibration phenomena investigated here are caused by self-excitation based on the friction forces between pad and disk or drum, see e.g. [50]. Particularly brake squeal represents this kind of noise phenomenon in the audible frequency range between 1 and 15 kHz, see e.g. [23]. Results regarding the influence of damping on high frequency brake vibrations have already been published in [16]. In general, models for brake squeal are nonlinear. For describing this phenomenon these models have to contain the self-excitation mechanism caused by the non-conservative friction forces and nonlinearities for restricting the vibrations to a limit cycle. The experimentally observed stationary vibration often possesses a dominant frequency during squeal, e.g. [17].

In practice, it is still state of the art to use linearized models around a stationary solution for describing the potential for brake squeal. Thereby the instability of the desired quiet solution is interpreted as squeal. If brake squeal models are linearized

D. Schmid (✉) · N. Gräbner · U. Wagner
Technische Universität Berlin, Einsteinufer 5, 10587 Berlin, Germany
e-mail: dominik.schmid@tu-berlin.de

N. Gräbner
e-mail: nils.graebner@tu-berlin.de

U. Wagner
e-mail: utz.vonwagner@tu-berlin.de

V. Mehrmann
Technische Universität Berlin, Straße des 17. Juni 136, 10623 Berlin, Germany
e-mail: mehrmann@math.tu-berlin.de

with respect to stationary operation states, the resulting equations of motion can be written as

$$\mathbf{M}\ddot{\mathbf{y}} + (\mathbf{D} + \mathbf{G})\dot{\mathbf{y}} + (\mathbf{K} + \mathbf{N})\mathbf{y} = \mathbf{0}, \quad (1)$$

with a symmetric and positive definite mass matrix \mathbf{M} , symmetric and positive semi-definite damping matrix \mathbf{D} and stiffness matrix \mathbf{K} as well as a skew-symmetric gyroscopic matrix \mathbf{G} and a circulatory matrix \mathbf{N} , while \mathbf{y} is the vector of displacement or rotation angles which can either result from FE models oder models with a low number of degrees of freedom, e.g. Multibody systems (e.g. [17]).

Fundamental properties of self-excited systems like stability and bifurcation behavior are strongly influenced by dissipation which therefore in general might have a decisive influence on noise and vibrations. More precisely, damping is capable to suppress vibrations but also to excite vibrations in self-excited systems, see e.g. [19]. The general influence of damping on brake models is investigated in [16]. Despite its general importance, damping mechanisms are often omitted or only very fundamentally considered in state of the art simulations both in industry and academia. A quantitative modeling is difficult due to scattering or a lack of parameters. The objective of the current investigations is to optimize the vibration behavior of brakes—following directly the title of the priority program—with respect of being calm and smooth by using deliberately introduced damping. This contribution shows results achieved in both phases of the project. In the first period the focus was on the investigation of damping influence of shims in disk brakes while the second period investigates more general the influence of related damping devices on drum brakes. Results regarding disk brake investigations are taken from the corresponding doctoral thesis [37]. Essential analytical, numerical as well as experimental outcome is shown subsequently, see more detailed results in the corresponding Sects. 4, 5 and 6 in [37]. Furthermore, results for a model of a duplex drum brake have already been presented in [45]. A modified FE model of a simplex drum brake, where one brake shoe acts as leading and the other as trailing shoe is shown below describing the experimentally investigated drum design in a more realistic manner.

The paper is organized as follows. First, shims, thin composite structures consisting of elastic and viscoelastic layers applied on brake pad back plates, are modeled and investigated experimentally. These investigations especially consider methods for Finite Element (FE) models regarding a homogenization process for multilayer shim compounds. Furthermore, different shim set-ups are tested for achieving maximum damping and studying the influence on the investigated brake system. In next steps, shims are applied to back plates as well as modified disks to assess the squealing behavior using a dynamometer test rig. The second part deals with the investigation of possibilities to include damping mechanisms in drum brakes. The focus is on damping devices capable to be fixed on the free surfaces of shoes (inner surface) and drum (outer surface). Especially the drum with its large free outer surface offers new possibilities compared to disk brakes. Experimental modal analyses of drum brake components are carried out. Furthermore, a Finite-Element drum brake model with respect to squeal is built up focusing on essential brake parts and damping measures.

2 Shims: Principle, Application and Modeling

In disk brakes thin shim structures are often applied on pad back plates as shown in Fig. 1a in order to avoid brake noise. Their layer thicknesses usually are in the range of a few tenths of a millimeter and they are intended for increasing damping or changing other dynamic properties. Figure 1b depicts the shim configuration used for the entire investigations. Here, a steel core is wrapped with two elastomer layers.

Currently in industrial applications, selecting appropriate shims requires a variety of tests. In the present investigations, the influence of essential factors like geometrical dimensions and rheological properties is considered systematically based on corresponding shim models. In FE-systems the modeling of thin shim composites in general is not easy. Often a multi-layer approach is used considering each layer individually [29]. This approach can cause large element distortions and reduce the quality of results in simulations strongly. Furthermore, modeling of damping—the key feature of shims—is often neglected completely leading to inaccurate computations. Besides sufficient damping often low weight and high static stiffness characteristics are required as well [20]. So, the aim of the actual investigations is to get a manageable modeling of the shims including all relevant effects for the considered brake vibrations.

In general shims possess a multi-layer structure. The damping increase of brake pads using shims is mainly based on the properties of the thin elastomer layers. A deformation of the pad compound due to bending shown in Fig. 2 results in a shearing behavior of the soft viscoelastic core. This shear deformation contributes to a much greater dissipation of brake pads. The principle applied here is called *Constrained-layer-damping* (CLD), where a thin damping core, often an elastomer, is placed between a stiff constraining layer and a thick carrier structure (beam).

Usually the beam possesses a much larger thickness than all additional layers affecting the stiffness of the entire CLD structure. Note that the main effect of shims may not consist in providing additional damping but rather pursues the increase of the pad stiffness [15]. Additional elastomer top (constraining) layers of shims can be described by the *Free-layer-damping* (FLD) concept [32]. FLD is a simple measure for damping of flexural vibrations. Therefore, a damping layer is applied to the structural surface to be damped. Similar to the just mentioned CLD compound, energy is dissipated by cyclic deformation of the structure, but in this context primarily by

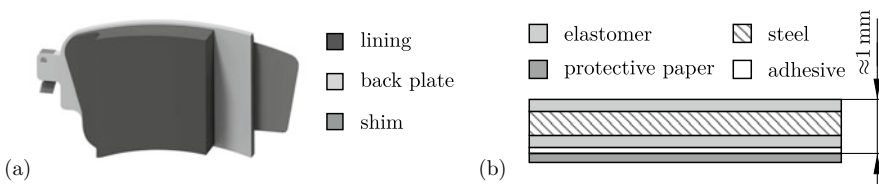


Fig. 1 a Typical brake pad composition [36] and b shim structure used for the investigations according to [37, 52][Fig.2.2]

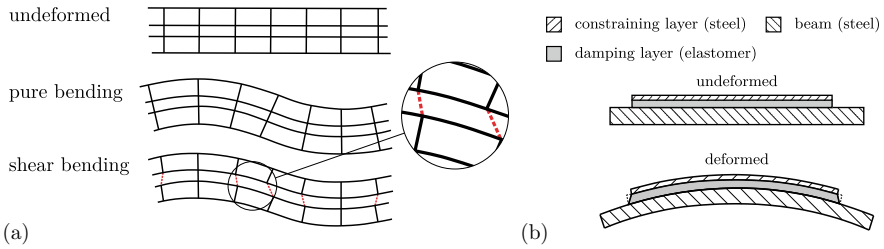


Fig. 2 a Shear deformation of viscoelastic core [43] according to [41, Fig. 5], [25, pp. 31] and b CLD mechanism according to [35],[pp. 62], see [37],[Fig.4.8]

elongation and contraction of the viscoelastic damping material [3, 22], not by shear. This damping principle has shown to be less effective on component level since there only has been a limited increase of damping. These elastomer top layers are intended primarily for affecting the contact between pad and piston respectively carrier during braking and contribute to an improved noise behavior.

Subsequently, analytical approaches are presented allowing the consideration of damping in CLD structures. A homogenization approach is used combining essential layers of the shim and providing equivalent system properties. The homogenized shim structure is implemented into an existing FE model of the overall brake system and validated using measurement data. The objective is to achieve equivalent system properties of the multi-layer CLD structure by just using one layer in the FE model.

In the following a homogenization method for a CLD assembly is presented based on the approaches from NASHIF et al. [31] and ROSS et al. [35]. Using the theory from ROSS the result is a homogenized stiffness parameter used for subsequent FE-simulations. The theory was originally developed for a rectangular cross-sectional composite while in general brake pad shims do not have a rectangular shape. Results of the present investigations for rectangular plates as well as brake pad back plates bonded with shims have already been published in [42] containing also experimental investigations. Due to a more complex geometry of pad back plates more iterations are needed to achieve a comparable match with experimental results as for rectangular plates. An additional analytical approach based on [24, 34] is used for considering essential parameters like shim length and layer thickness particularly affecting damping of shim composites. This theory describes lateral vibrations of a three layer CLD structure. Natural frequencies and loss factors [10, 48] of each bending mode can be determined for the compound, see results in [39]. The damping results from the shearing of the viscoelastic core is mapped by the elastomer loss factor. Results based on the presented theories for variations of the shim coverage are shown in Fig. 3 comparing a symmetrical application in (a) and an edge application starting at $x = 0$ in (b).

It is clearly visible that there is a dependency of the loss factor maximum on the bending mode as well as the degree of coverage. Considering a symmetrical application the first mode shape shows the highest loss factor at approximately 50% coverage whereas the maximum at higher modes moves more and more towards a

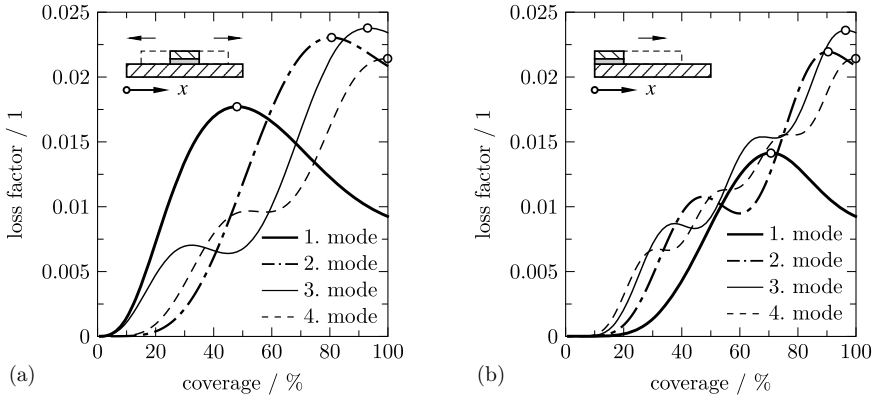


Fig. 3 Influence of shim length considering a rectangular CLD structure ($180 \times 50 \times 5 \text{ mm}^3$) on **a** symmetrical application [37][Fig. 4.16 a] and **b** application at $x = 0$ [37],[Fig. 4.17 a]

fully covered carrier structure. Considering the configuration in (b) a much higher coverage tends to be needed for achieving an equivalent damping potential.

Summarizing, the following aspects can be noted. First of all, it is of relevance to have knowledge about what mode shape shall be damped preferably because there is a strong dependency on system properties.

- A maximum loss factor of the shim is not always the primary design goal. Stiffness and mass distribution often play a decisive role, see mode decoupling scenarios [27].
- The selection of the damping material is essential. Good dissipation properties over a wide temperature and frequency range are desirable, see dynamic-mechanical analysis and modal analysis carried out in [38, 40].
- Increasing the stiffness and thickness of the constraining layer as well as using elastomers with a high loss factor have proven to be effective [13, 22]. Partial coverage can lead to higher as well as lower loss factors and should be taken into account when selecting shims. Therefore it can not be assumed that an increase of the shim length contributes to larger loss factors.
- An additional fixation of shims with the back plate by riveting should be avoided to achieve the highest possible damping.

Experimental tests on component level considering temperature influence as well as coverage variation and delamination scenarios have been carried out in [37, 38, 40]. Support has been provided by student workers [4, 7, 11, 12, 26, 47] and [9] on specific modeling and experimental aspects during the project, see [37]. Furthermore, the homogenization approach used has been validated in [42]. The results showed a very good agreement with experimentally determined natural frequencies by simultaneously maintaining all mode shape as well as the order of appearance. The reference to damping is considered later in Sect. 4.

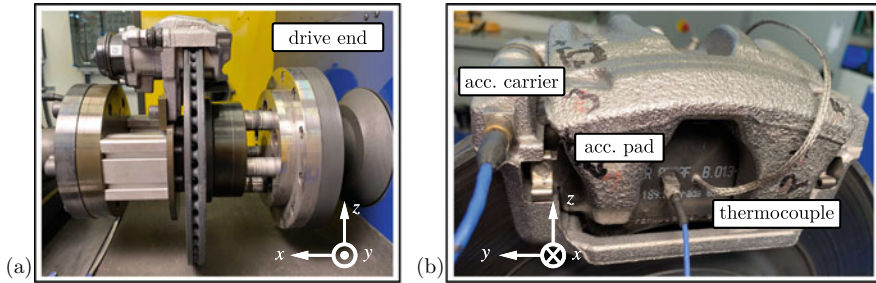


Fig. 4 **a** Investigated floating caliper brake and **b** positioning of triaxial accelerometers and thermocouple [37],[Fig. 5.17]

3 Brake Set-up

The industrial floating caliper brake shown in Fig. 4 is used for the entire experimental investigations. To measure time series during squealing two triaxial accelerometers are applied, placed on the caliper and shim as well as an external thermocouple for recording temperature. All test campaigns were carried out on a LINK dynamometer test rig D 1500 at Chair of Mechatronics and Machine Dynamics at Technische Universität Berlin.

To determine the influence of shims on brake noise, identical test campaigns were carried out for brake pads with shims and after removing shims. One test cycle included 180 brakings considering different pressure and speed levels. Test bench trials were repeated ten times to achieve a better quality of squeal information. Figure 5 shows the squealing frequencies determined from the time data.

Comparing both test scenarios it is obvious that applying shims contributes to a more silent brake system. Figure 5 clarifies that a lower number of squealing events, lower acceleration amplitude levels correlated with the volume of the perceived squealing noise and a lower number of squeal frequencies occurred using shims. However, there has been no complete elimination of squealing. It is noticeable that even a new squeal frequency with a dominating y-direction at 1.4 kHz appears, which was not present before. A damping increase due to shearing of the elastomer core requires an appreciable deformation of the pad. A reduction of noise by using shims is therefore often only noticeable for higher squealing frequencies.

The question therefore is, if damping devices can be applied more efficiently with respect to the avoidance of squeal. This has led to tests of further measures. We hereby focused on the damping of the gray cast brake disk. The intention by these investigations was not primarily to find a countermeasure directly applicable in real brakes, but to get basic insights into the effectiveness of damping of components on the behavior of the overall system. In WEHNER et al. [51] it has been proved theoretically using a FE model, that damping of the disk is very effective (and much more effective than damping pads) with respect to the avoidance of squeal. According to [8], the friction rings of the disk (i.e. the part in contact with the pad) account for the

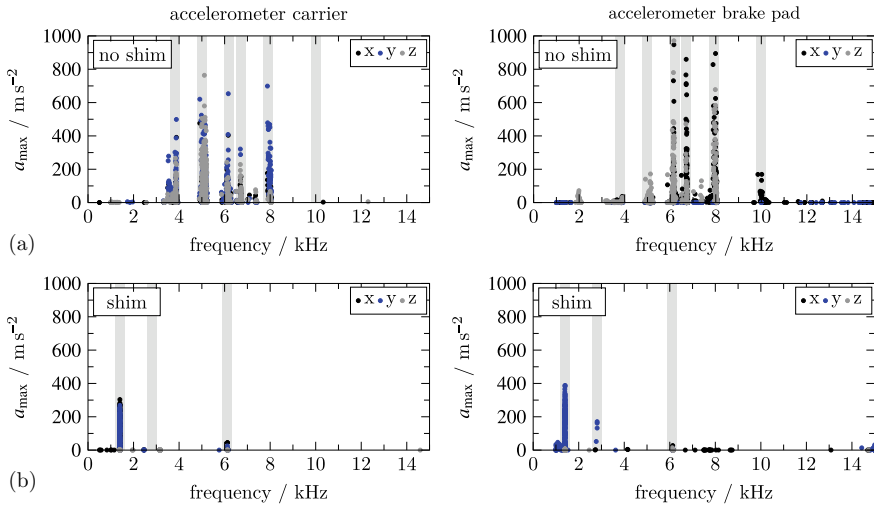


Fig. 5 Maximum acceleration a_{max} measured during squealing: brake pads **a** without shims and **b** using shims [37],[Fig.5.21]

largest part of noise radiation, approximately about 70%. Unfortunately modifying disks is often a demanding task for thermal and safety reasons. In our tests the outer cooling fins were removed as depicted in Fig. 6 and shims were positioned inside the groove and along the circumferential surface. As already mentioned these measures are not directly applicable to series and have exclusively been used for our academic trial purposes.

On component level experimental modal analysis were carried out for both test set-ups, brake disk with and without shims. All measurement objects were placed on soft foam to realize a free-free equivalent support. For excitation an automatic impulse hammer and for measuring the output signal a laser vibrometer have been applied. The frequency response functions are shown in Fig. 6.

The shims used ensure that there is a reduction of peak amplitudes particularly in the frequency range above 3 kHz. Table 1 provides information about the first eigen shapes considering the response behavior. Comparing damping ratios determined from transfer functions of the modified disk and shims used by default on back plates show that there is a lower damping characteristic for the modified disk. However, a closer look clarifies a significant increase in damping compared to conventional grey cast iron brake disks possessing damping ratios in the order of 0.001 and below. Additionally as argued before, a larger influence of disk damping on the noise problems is expected, especially in the lower frequency range.

In fact, dynamometer testing emphasizes how effective the measure is, as shown in Fig. 7. The detected squeal distribution is compared subsequently. Each marker correlates with a squealing event measured. Shims placed on disk brakes increase the damping capacity significantly and show a clear benefit on the noise behavior.

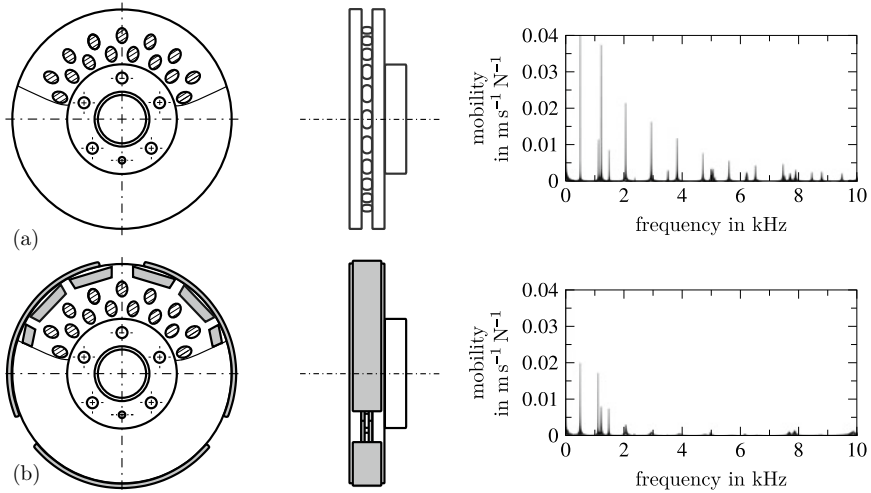


Fig. 6 Modifications of brake disk in order to investigate measures to increase damping. Corresponding mobility (free-free support): **a** disk with removed outer cooling fins and **b** disk with removed outer cooling fins and added shims in groove and along circumference [37],[Fig. 5.14]

Table 1 Influence of shims on system properties of brake components: free-free supported modified brake disk and back plate applied with shims [37],[Table 12], [37][Table 18]

	f_1 Hz	ϑ_1 –	f_2 Hz	ϑ_2 –	f_3 Hz	ϑ_3 –	f_4 Hz	ϑ_4 –	f_5 Hz	ϑ_5 –
Disk	518	0.005	1130	0.001	1231	0.005	1497	0.002	2078	0.008
Back plate	2475	0.009	3548	0.008	5817	0.007	7622	0.006	9755	0.005

f —natural frequency, ϑ —damping ratio

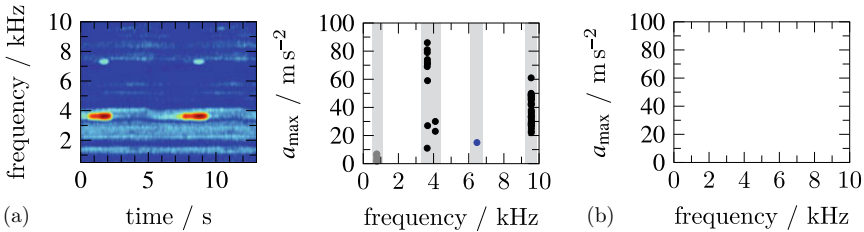


Fig. 7 Spectrogram of acceleration signals and overview of occurring squealing frequencies: **a** squeal events detected for brake disk without shims and **b** no squeal events occurred for brake disk using shims [37],[Fig. 5.27]

The squeal affinity could be reduced entirely by the tested measures. As a result, additional damping measures should focus on increasing the damping of the disk which is not an easy task to realize in serial mass produced specimen.

4 Finite-Element Modeling

Shims are inevitably a problem when modeling via Finite-Element programs due to very thin layers. A finer meshing and thus an increase of degrees of freedom is not desired for complex brake models and contributes to significantly longer computation times. Experimental modal analyses of identical brake pads have shown that there is a non-negligible variation especially in damping characteristics [37]. Therefore, the mapping of damping has to be considered within suitable tolerances in simulations. While implementing damping, the choice of Rayleigh-damping [5] seems to be the most appropriate one. This kind of damping gives a sufficiently precise characterization of the dissipation behavior in the squeal relevant range considering the variation captured in test set-ups. FE computations at component level of homogenized shim structures in [42] showed a very good agreement with experimental tests. The damping therein has been mapped realistically as well as the natural frequencies. The shim homogenization process has shown to obtain equivalent results and has been used subsequently for implementation in an already existing industrial FE brake model of the experimentally examined brake.

The state of the art in squeal simulations in industry is to perform the so-called Complex Eigenvalue Analysis (CEA). For CEA the eigenvalues of the brake system are computed. Due to the friction forces between pad and disk asymmetries in the displacement proportional terms, i.e. a stiffness matrix and a circulatory matrix, and additionally gyroscopic terms, eigenvalues with positive real parts $\text{Re}(\lambda)$ are possible, see e.g. [17, 33]. This means that the trivial solution of the (with respect to an equilibrium position linearized) equations of motion becomes unstable and the corresponding vibration mode and frequency are considered to belong to potential corresponding squeal. A comparison is made between a conventional multi-layer shim approach in (b) and a homogenized shim compound in (c), see Fig. 8. For validating the simulation results squeal events measured have been considered in (a).

Comparing the two approaches in (b) and (c) a clear difference can be seen. The conventional multi-layer approach in (b) shows a poorer agreement with the experimentally determined squealing events in the frequency range up to 10 kHz, while also (c) only determines some of the experimentally found squealing frequencies. When examining the deformation behavior of mode shapes in (b) large element distortions occurred locally due to the thin element thicknesses, see results in [37]. These (unphysical) distortions [30] may lead to (also unphysical) positive real parts and therefore worsen the quality of the results. However, the homogenized shim approach in (c) constitutes a significant improvement in modeling [37]. As a result, realistic mode shapes can be observed as well as squeal frequencies are mapped in a much better way especially at 4 kHz and 6 kHz.

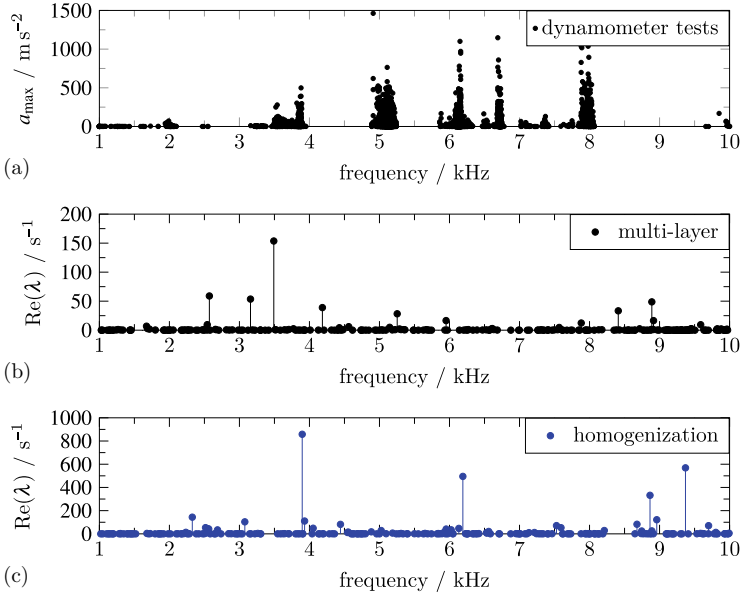


Fig. 8 Validation of squeal events: **a** dynamometer tests and results of CEA: **b** multi-layer and **c** homogenized shim approach [37],[Fig. 6.8]

To reduce computation time in multi-parameter simulations and complex eigenvalue analysis, model reduction methods for the associated FE models have been developed and implemented as Python and Matlab codes in the first project phase [18]. These methods were employed in [6] to develop homotopy methods. By first reformulating the second order system (1) as a first order perturbed dissipative Hamiltonian system $E\dot{z} = (J - R_D)z - R_N z$, with

$$J := \begin{bmatrix} -G & -(K + \frac{1}{2}N) \\ (K + \frac{1}{2}N^T) & 0 \end{bmatrix}, \quad (2)$$

$$E := \begin{bmatrix} M & 0 \\ 0 & K \end{bmatrix}, \quad R := R_D + R_N = \begin{bmatrix} D & 0 \\ 0 & 0 \end{bmatrix} + \begin{bmatrix} 0 & -\frac{1}{2}N \\ -\frac{1}{2}N^T & 0 \end{bmatrix}, \quad (3)$$

one sees that the circulatory term N associated with the FE nodes on the contact surface is solely responsible for the eigenvalues with positive real part, since the system with $N = 0$ always is Lyapunov stable, i.e. it has a spectrum in the closed left half plane [28] with all eigenvalues on the imaginary axis being semisimple.

Using a full scale industrial FE model and bringing in the perturbation term $R_N Q$ via a homotopy $E\dot{z} = (J - R_D)z - \alpha R_N z$, $\alpha \in [0, 1]$. it was observed that for $\alpha = 0$ the maximum real part is $-5.0462e - 06$ and for $\alpha = .1$ it is already $2.0336e - 05$, see Fig. 9, where the largest real part of an eigenvalue is plotted vs. the parameter α , i.e. the unperturbed problem is already close to instability under unstructured perturbations.

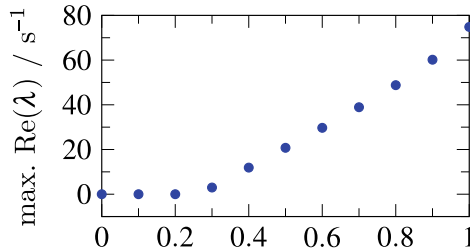


Fig. 9 Eigenvalue plot for $\alpha \in [0, 1]$ [6] [Fig.4.1]

In order to decide already in a design phase whether the norm of the matrix N is tolerable to preserve the asymptotic stability in [2] a new efficient method was developed to determine the structured distance to instability for large scale problems and to determine the imaginary part of the eigenvalue, where the eigenvalue is crossing the imaginary axis. The method combines nonlinear eigenvalue optimization methods with the described model reduction methods.

5 Investigations on Drum Brakes

Drum brakes have largely disappeared in passenger cars in the last years. However, this type of friction brake is returning in terms of the emergence of electrically powered vehicles and particle emissions. When used, drum brakes are often applied within the rear-axels in cars [1] and in buses or trailers [21]. Generally, electric vehicles are in wide operational states decelerated using the regenerative brake of the electric motor additionally to friction brakes. The consequence is that conventional brake systems are no longer permanently exposed to wear. For this reason, drum brakes are being used more and more frequently at least for rear-axles. Lower costs in general [14] and the reduction of abrasion emissions due to the encapsulated design [49] are two main advantages compared to disk brake systems. Nevertheless, noise in the audible frequency range remains during braking, particularly before standstill.

Usually, industrial drums consist of cast material possessing a high damping potential among other suitable mechanical properties [14]. These industrial brakes are often optimized in such way that there are almost no squealing events occurring in academic test series. To investigate the influence of damping a steel drum, manufactured at the Chair of Mechatronics and Machine Dynamics, instead of gray cast iron is used for all further investigations presented here. This steel drum possesses a much lower material damping than cast materials. The simpler structure neglecting cooling fins also simplifies the Finite-Element modeling. A steel drum with an outer diameter of 214 mm has been turned from a hollow steel cylinder and has been used entirely for research purposes.

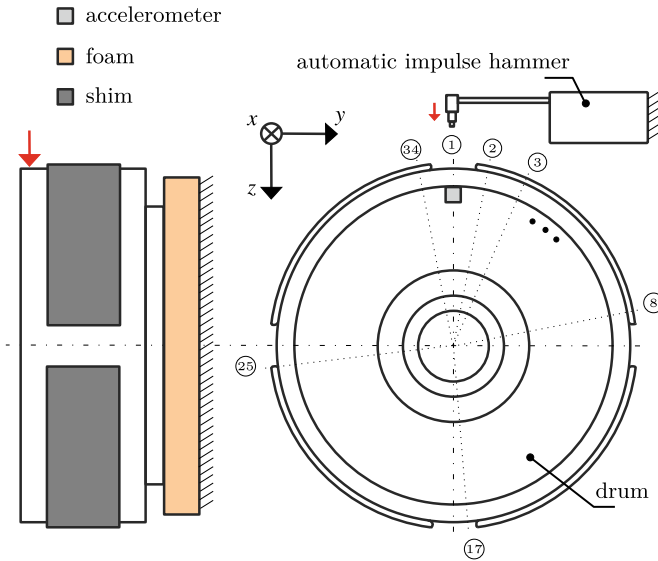


Fig. 10 Modal analysis set-up of non-industrial steel drum considering 34 collocation points [44] and [45] [Fig. 3]

Table 2 Damping ratios of non-industrial steel drum, [45, Table 2]

	ϑ_1 %	ϑ_2 %	ϑ_3 %	ϑ_4 %	ϑ_5 %	ϑ_6 %	ϑ_7 %	ϑ_8 %	ϑ_9 %
No shim	0.057	0.070	0.079	0.061	0.030	0.210	0.019	0.232	0.135
Shim	0.252	0.424	0.703	0.632	0.351	0.841	–	0.831	0.568
Increase	342	506	790	936	1070	300	–	258	320

ϑ —damping ratio

Results showing CEA of a modified duplex drum brake have already been described in [45]. The modeling and outcome presented herein correspond to the real simplex drum brake also experimentally investigated at the Chair of Mechatronics and Machine Dynamics. For increasing the dissipation of the drum, four rectangular shim plates (width length 53 mm, length 139 mm) are applied along the circumference equidistantly. For determining system properties like natural frequencies and damping ratios of brake components the modal analysis set-up shown in Fig. 10 is used.

Damping ratios ϑ for both drum set-ups—with and without shims - are shown subsequently in Table 2. Adding shims results in an increase in damping caused by the CLD mechanism as described priorly. Damping ratios are about 3 to 10 times larger than in the turned steel drum. Missing values in Table 2 and 3 could not be determined in the applied evaluation procedure.



Fig. 11 Industrial brake shoe attached with shims investigated in [9]

Table 3 Damping ratios of industrial brake shoes, data from [9, Table 4.4]

	ϑ_1 %	ϑ_2 %	ϑ_3 %	ϑ_4 %	ϑ_5 %	ϑ_6 %	ϑ_7 %	ϑ_8 %
No shim	–	0.6	0.6	0.6	0.4	–	0.6	0.8
4 shims	0.9	1.4	1.6	2.1	1.4	–	–	1.5

ϑ —damping ratio

Besides the drum surface passive damping structures like shims can be attached to brake shoes as well which has been investigated in the student thesis [9]. One version tested therein is visible in Fig. 11.

The damping ratios of the variant that have shown in [9, Table 4.4] the biggest impact on damping is summarized in Table 3. Damping ratios of the measure are compared with the industrial brake shoe. The lining itself contributes to a relatively high damping potential of approximately 0.6 %. Adding shims increases the damping of the brake shoes once again significantly, especially in the tested partial coverage execution.

The tests yield that these two placements (drum and shoes) show a considerable potential for increasing damping. Future tasks might deal with e.g. how to apply them in vehicles.

The FE modeling of the drum brake in Fig. 12 concentrates on fundamental components like drum and brake shoes including lining. All components are modeled with a simplified geometry. The focus is rather how damping can influence the noise behavior of drum brakes in general. Hexahedral solid elements with a quadratical approach (C3D20) are used for meshing all brake parts. Reference points positioned near the brake shoes and the center of the drum allow the application of concentrated forces and bearings (pinned-pinned) as well as pivot of the brake parts. The results presented below relate to the simplex drum brake configuration in Fig. 12, where one brake shoe acts as leading shoe and the other as trailing shoe. The contact between lining and drum is based on a surface to surface formulation. Steel components like drum and back plate are modeled using isotropic properties. For modeling shims a homogenization approach is used. The lining consisting of several components [46] shows a nonlinear and transversal isotropic material behavior [53]. Direction-dependent parameters for the friction material are implemented using engineering constants.

The approach is rather to show where damping is particularly effective. For these positions, damping is implemented in a realistical manner using Rayleigh parameters

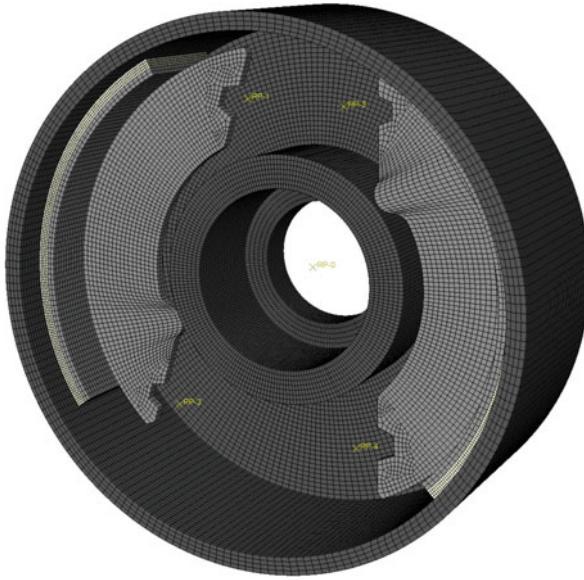


Fig. 12 FE drum brake model

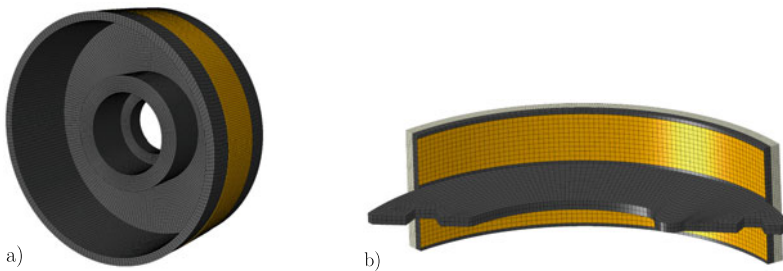


Fig. 13 Shims applied to: **a** drum surface and **b** brake shoes

determined from experimental damping ratios, see Table 3. A discussion on a higher term approach like using a Caughey series has been investigated in [45]. The Rayleigh parameters are implemented in all shim components as well as the drum and brake shoes. A shim ring with a width of 40 mm and a thickness of 1 mm is attached to the outer surface of the drum via tie-constraint. Each brake shoe is equipped with two shims filling the given space. A detailed view of the brake components including shims is shown in Fig. 13.

The results of CEA are summarized in Fig. 14. The eigenvalues show that damping the outer surface drum contributes to an improvement in noise behavior. Much fewer eigenvalues show a positive real part in the investigated frequency range. Shims applied on brake shoes show a high effectiveness in the frequency range above 5 kHz.

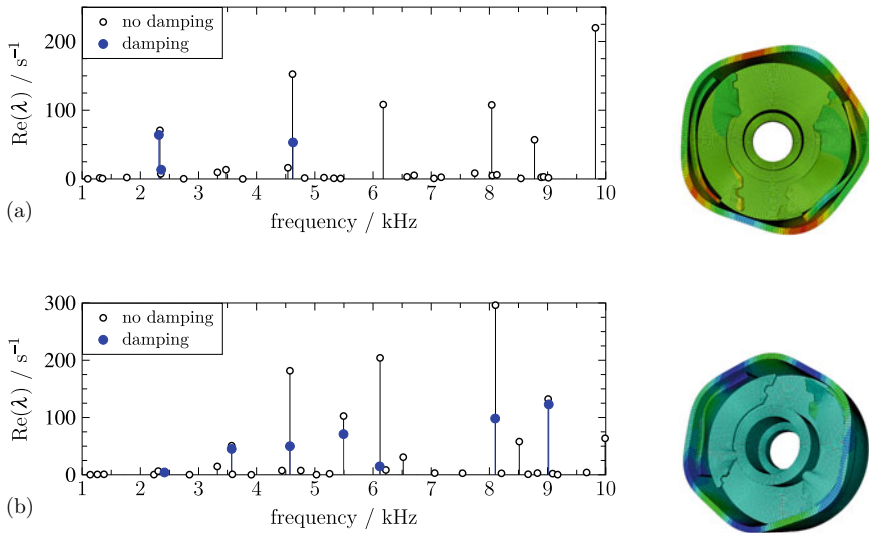


Fig. 14 Results of CEA considering damping in: **a** brake shoes (mode shape at 4616 Hz) and **b** drum (mode shape at 6121 Hz)

All positive real parts have been shifted successfully in the negative half-plane in this frequency range.

Nevertheless, there are still three positive real parts in the lower frequency range remaining. Therefore, it can be stated that damping the drum and brake shoes are one of the key aspects for reducing or even preventing squeal in the future. A combination of both measures should be aimed to achieve silent drum brakes. Note that additional masses and the overall stiffness influence the entire brake system.

A comparison with dynamometer tests considering the academic steel drum are intended to be focused in near future in a separate paper.

6 Conclusions

Within the actual DFG priority program “Calm, Smooth and Smart” countermeasures against high frequency brake vibrations were investigated. These vibrations are caused by self-excited vibrations, and this problem is a typical example of NVH issues in automotive industry. Countermeasures for disk as well as drum brakes were investigated in detail focusing on damping. Damping is well-known to be a powerful countermeasure against self-excited vibrations, if applied appropriately. In the first project period thin composite structures, called shims, were examined. As a result an improved approach for the FE-modeling of shims based on homogenization was developed. Further key aspects that have emerged can be summarized as follows:

- A dynamic characterization of shims is important to obtain damping properties and to classify the vibration behavior in the squeal relevant frequency range. This includes both the determination of the damping potential of viscoelastic elastomers within the essential temperature and frequency range as well as modal properties. Furthermore, the shim length and positioning plays a decisive role for achieving a maximum damping effect for the considered configuration. The investigations showed that increasing the shim length does not necessarily contribute to greater damping ratios.
- The FE modeling of shims as homogenized equivalent single-layer structure provides adequate aspect ratios of the elements, prevents strong elemental distortions and therefore shows a realistic deformation behavior. Besides these central aspects this type of modeling provides a reduction of degrees of freedom and leads to more efficient computation times. In Complex Eigenvalue Analysis the homogenized shim structure showed a better agreement with dynamometer tests carried out than the conventional used multi-layer approach.
- For eliminating low-frequency squealing the increase of brake disk damping has shown to be essential. The friction ring surfaces of the disk are usually responsible for a large part of sound radiation. In test set-ups a completely silent disk brake has been achieved by positioning shims instead of the outer cooling fin ring and towards the circumferential direction.
- Damping the drum as well as the brake shoes is one of the key measures for achieving silent drum brakes. Experimental modal analysis showed a significant increase in damping when applying shims on both surfaces. The Complex Eigenvalue Analysis for the developed drum brake model considering the essential brake parts confirmed this.

Acknowledgements This work is funded by the Deutsche Forschungsgemeinschaft (DFG, German Research Foundation) WA1427/27-1,2, project number 314964071 and ME790/36-1,2 “Suppressing brake vibrations by deliberately introduced damping” within the PP 1897 “Calm Smooth and Smart - Novel Approaches for Influencing Vibrations by Means of Deliberately Introduced Dissipation.” We would also like to thank Audi AG, Wolverine Advanced Materials and AL-KO Kober SE for their support.

References

1. Ahmed, I.: Modeling of vehicle drum brake for contact analysis using ansys. SAE Technical Paper 2012-01-1810 (2012)
2. Aliyev, N., Mehrmann, V., Mengi, E.: Computation of stability radii for large-scale dissipative Hamiltonian systems. *Adv. Comput. Math.* **46**, 6 (2020)
3. ASTM E 756-05: Standard test method for measuring vibration-damping properties of materials, 10-2005, pp. 1–14 (2005)
4. Bartholomäus, T.: Erstellung einer MATLAB-Routine zur automatisierten Dämpfungsbestimmung. Bachelorarbeit, MMD, TU Berlin (2017)
5. Bathe, K.J., Wilson, E.L.: Numerical Methods in Finite Element Analysis. Prentice-Hall, New Jersey (1976)

6. Beckesch, A.: Pfadverfolgung für Finite-Elemente-Modelle parametrischer mechanischer Systeme, Master Thesis, TU Berlin, 2018
7. Bökemeier, L.: Untersuchungen des Einflusses von Nichtlinearitäten und Temperatur auf Systemeigenschaften von Bremsbelägen. Bachelorarbeit, MMD, TU Berlin (2017)
8. Buck, A.: Simulation von Bremsquietschen (Brake Squeal), Dissertation TU München (2008). Shaker Verlag, Aachen
9. Conrad, J.: Bestimmung modaler Eigenschaften von Trommelbremskomponenten und Erprobung von Maßnahmen zur Dämpfungserhöhung, Bachelor thesis, MMD, TU Berlin, 2019
10. Cremer, L., Heckl, M.: Körperschall. Springer, Berlin Heidelberg New York (1967)
11. Dannwolff, H.: Analytische Ermittlung von Shimverlustfaktoren unter Verwendung von Constrained-layer-damping Theorien. Masterarbeit, MMD, TU Berlin (2018)
12. Exposito, S.C.: Untersuchung zum Quietschen von Trommelbremsen. Bachelorarbeit, MMD, TU Berlin (2018)
13. Flint, J.: Disc Brake Squeal, Dissertation University of Southern Denmark Engineering College of Odense. Vester Kopi (2002)
14. Ganguly, S., Tong, H., Dudley, G., Connolly, F., Hoff, S.: Eliminating drum brake squeal by a damped iron drum assembly. SAE Technical Paper 2007-01-0592, pp. 1–10 (2007)
15. Glisovic, G., Miloradović, D.: Eliminating brake noise problem. *Int. J. Mobil. & Veh. Mech.* **36**(3), 37–51 (2010)
16. Gräbner, N., Gödecker, H., von Wagner U.: On the Influence of Damping on Brake Vibrations. International Conference on Engineering Vibration, pp. 1–11 (2015)
17. Gräbner N.: Analyse und Verbesserung der Simulationsmethode des Bremsenquietschens, Dissertation TU Berlin, 2016
18. Gräbner, N., Mehrmann, V., Quraishi, S., Schröder, S.: von Wagner, U: Numerical methods for parametric model reduction in the simulation of disc brake squeal. *Zeitschrift für Angewandte Mathematik und Mechanik.* **96**, 1388–1405 (2016)
19. Hagedorn, P., Heffel, E., Lancaster, P., Müller, P.C., Kapuria, S.: Some recent results on MDGKN-systems. *ZAMM* **95**(7), 695–702 (2015)
20. Hajela, P., Lin, C.-Y.: Optimal design of viscoelastically damped beam structures. *Appl. Mech. Rev.* **44**(11) Part 2, 96–106 (1991)
21. Hamid, M.N.A., Teoh, C.-Y., Ripin, Z.M.: The operational deflection shapes and transient analysis of the brake shoes in drum brake squeal. *Proc. Inst. Mech. Eng. Part D J. Automob. Eng.* **227**(6), 866–884 (2013)
22. Kerwin, Jr. E.M., Ungar, E.E.: Requirements imposed on polymeric materials by structural damping applications. In: Corsaro, R.D., Sperling, L.H. (eds.) *Sound and Vibration Damping with Polymers*. ACS Symposium Series, vol. 424, pp. 317–345 (1990)
23. Kinkaid, N.M., O'Reilly, O.M., Papadopoulos, P.: Automotive disc brake squeal. *J. Sound Vib.* **267**(1), 105–166 (2003)
24. Lall, A.K., Asnani, N.T., Nakra, B.C.: Damping analysis of partially covered sandwich beams. *J. Sound Vib.* **123**(2), 247–259 (1988)
25. Lazan, B.J., Metherfell, A.F., Sokol G.: Multiple-band surface treatments for high damping. Technical Report AFML-TR-65-269, pp. 1–45 (1965)
26. Maaß, C.: Einfluss von Klebstoffschichten auf Verlustfaktoren eines Constrained-layer-damping Aufbaus und Ermittlung von Streuungskenngrößen bei Bremsbelägen. Bachelorarbeit, MMD, TU Berlin (2019)
27. Mead, D.J.: The practical problems of assessing damping treatments. *J. Sound Vib.* **1**(3), 270–291 (1964)
28. Mehl, C., Mehrmann, V., Wojtylak, M.: Linear algebra properties of dissipative Hamiltonian descriptor systems. *SIAM J. Matrix Anal. Appl.* **39**, 1489–1519 (2018)
29. McDaniel, J.G., Li, X., Elvenkemper, A., Wegman, E., Wang, A., Chen, S.E., Flint, J.: Simulating the effect of insulators in reducing disc brake squeal. SAE Technical Paper 2005-01-3944, pp. 1–7 (2005)

30. Morris, A.: *A Practical Guide to Reliable Finite Element Modelling*. John Wiley & Sons Ltd., Chichester (2008)
31. Nashif, A.D., Jones, D.I.G., Henderson, J.P.: *Vibration Damping*. John Wiley & Sons, Chichester (1985)
32. Oberst, H., Frankenfeld, K.: Über die Dämpfung der Biegeschwingungen dünner Bleche durch fest haftende Beläge. *Acta Acustica united with Acustica* **2**(4), 181–194 (1952)
33. Popp, K., Rudolph, M.: *Brake Squeal, Detection, Utilization and Avoidance of Nonlinear Dynamical Effects in Engineering Applications Final Report*, pp. 197–225. Shaker Verlag, Aachen (2001)
34. Rao, D.K.: Frequency and loss factors of sandwich beams under various boundary conditions. *J. Mech. Eng. Sci.* **20**(5), 271–282 (1978)
35. Ross, D., Ungar, E., Kerwin, Jr. E.M.: Damping of plate flexural vibrations by means of viscoelastic laminae. In: Ruzicka, J.E. (eds.) *Structural Damping*, pp. 49–87. Pergamon Press, New York (1959)
36. Schmid, D.: Brake pad. figshare. Dataset., Lizenz CC BY4.0 (2018). <https://doi.org/10.6084/m9.figshare.7046663.v1>. <https://figshare.com/articles/Brakepad/7046663>
37. Schmid, D.: Zum Einfluss von Dämpfung auf Bremsenschwingungen, Dissertation TU Berlin, Lizenz CC BY4.0, 2020
38. Schmid, D., Gräbner, N., von Wagner, U.: Experimental Investigations of Brake Pad Shim Properties. *Proceedings in Applied Mathematics and Mechanics*, vol. 17, No. 1, pp. 41–44. Wiley (2017)
39. Schmid, D., Gräbner, N., von Wagner, U.: Characterization of Brake Shims Using Analytical Constrained Layer Damping Theories. *Proceedings in Applied Mathematics and Mechanics*, vol. 18, No. 1, pp. 1–2. Wiley (2018)
40. Schmid, D., Sessner, V., Gräbner, N., von Wagner, U., Weidenmann, K.A.: Parameter Identification of Brake Pad Shims for Complex Eigenvalue Analysis. *Proceedings in Applied Mathematics and Mechanics*, vol. 19, No. 1, pp. 1–4. Wiley (2019)
41. Parfitt, G.G., Lambetz, D.: The damping of structural vibrations, C. P. No. 596 Aeronautical Research Council. Her Majesty's Stationery Office, London (1962)
42. Schmid, D., Gräbner, N., von Wagner, U.: On brake pad shim characterization: a homogenization approach and finite element analysis. In: *Advanced Structured Materials—New Achievements in Continuum Mechanics and Thermodynamics*, vol. 108, pp. 447–464. Springer (2019)
43. Schmid, D.: Constrained-layer-damping shear bending. figshare. Figure, Lizenz CC BY4.0 (2019). <https://doi.org/10.6084/m9.figshare.8143808.v1>. https://figshare.com/articles/Constrained-layer-damping_shear_bending/8143808
44. Schmid, D.: Modal analysis set-up of non-industrial steel drum. figshare. Figure, Lizenz CC BY4.0 (2022). <https://doi.org/10.6084/m9.figshare.17715890.v1>. https://figshare.com/articles/figure/Modal_analysis_set-up_of_non-industrial_steel_drum/17715890
45. Schmid, D., Gräbner, N., von Wagner, U.: Friction induced noise in drum brakes: finite-element modeling and experiments with special focus on damping. *Arch. Appl. Mech.* (2022)
46. Selamat, M.S.B.: Friction materials for brakes application. *J. Ind. Technol.* **14**(2), 9–25 (2005)
47. Seltitz, S.: Experimentelle Dämpfungsuntersuchungen an Bremsbelägen. Bachelorarbeit, MMD, TU Berlin (2016)
48. Ungar, E.E., Kerwin, E.M., Jr.: Loss factors of viscoelastic systems in terms of energy concepts. *J. Acoust. Soc. Am.* **34**(7), 954–957 (1962)
49. Vey, C., Pfeffer, P.E.: Brake systems 2025—Future Trends. In: *9th International Munich Chassis Symposium 2018*. Springer, Heidelberg, Dordrecht, London, New York (2019)
50. Wallaschek, J., Hach, K.-H., Stolz, U., Mody, P.: A survey of the present state of friction modelling in the analytical and numerical investigation of brake noise generation. In: *Proceedings of the ASME Vibration Conference DETC99/VIB-8357*, pp. 1–12 (1999)
51. Wehner, J.H., Jekel, D., Sampaio, R., Hagedorn, P.: Damping Optimization in Simplified and Realistic Disc Brakes. *Springer Briefs in Applied Sciences and Technology*, pp. 1–50 (2018)
52. Wolverine Advanced Materials, Shim datasheets (2016)
53. Yuhas, D.E., Ding, J., Venkatesan, S.: Non-linear aspects of friction material elastic constants. *SAE Technical Paper 2006-01-3193*, pp. 1–10 (2006)